Dielectric Behavior of Nonpolar Polymers and Their Composites: The Case of Semicrystalline Polyolefins

Stavros X. Drakopoulos, Sara Ronca, and Ignacio Martin-Fabiani

Abstract Polyolefins are thermoplastic polymers used in a wide range of applications, including medical implants, insulating materials, fabrics, and packaging. The two most popular representatives, polyethylene (PE) and polypropylene (PP), present linear chemical structures that yield these materials semicrystalline (except for atactic PP). The versatility of their synthesis enables the fabrication of different grades, covering a wide range of crystallinities which can reach up to 90%. However, because of their symmetric aliphatic structure, they do not present a permanent dipole moment. Their nonpolar nature makes dielectric spectroscopy measurements challenging, as this technique relies on the relaxation of dipoles after the application of an external electric field. Here, we review different approaches that have been followed in order to introduce permanent dipoles and render polyolefins dielectrically active, including: (i) addition of probes with a permanent dipole moment, (ii) oxidation/chlorination to produce dielectrically active chains, or (iii) induced oxidation in the presence of metal oxide fillers. The introduction of dipoles, either intentionally or due to the presence of impurities, has enabled the characterization of the full relaxation spectra of polyethylene and polypropylene as well as the assignment of dielectric relaxations to their respective molecular mechanisms. We then turn our attention into PE and PP composites for electrical energy storage and insulation applications. We show how, in these materials, the effect of the polymer matrix and filler orientation has been proven key to enhance their dielectric breakdown strength.

Keywords Polyolefins · Nanocomposites · Crystallinity · Orientation · Dielectric probes · Entanglement · Dielectric breakdown strength · Treeing

S. X. Drakopoulos · S. Ronca · I. Martin-Fabiani (✉)
Department of Materials, Loughborough University, Loughborough, Leicestershire LE11 3TU, UK
e-mail: i.martin-fabiani@lboro.ac.uk

T. A. Ezquerra and A. Nogales (eds.), *Crystallization as Studied by Broadband Dielectric Spectroscopy*, Advances in Dielectrics,
https://doi.org/10.1007/978-3-030-56186-4_10

Abbreviations

PE	Polyethylene
LDPE	Low density polyethylene
HDPE	High density polyethylene
UHMWPE	Ultra-high molecular weight polyethylene
PP	Polypropylene
i-PP	Isotactic polypropylene
TiO_2	Titanium oxide
Al_2O_3	Aluminum oxide
DBANS	4,4′-(N,N-di- butylamino)-(E)-nitrostilbene
MMT	Montmorillonite
o-MMT	Organo-montmorillonite
CNF	Carbon nanofibers
MWCNT	Multi-wall carbon nanotubes
$CaCO_3$	Calcium carbonate
$BaTiO_3$	Barium titanate

1 Introduction

The global plastic production has increased exponentially since 1950, when 1.5 tonnes were produced, rising to almost 348 million tonnes in 2017. In Europe alone, over 1.5 million people are directly employed in the 60,000 companies related to the plastic industry [1]. Polyolefins, consisting of saturated aliphatic hydrocarbon macromolecules, account for more than 55% of the global plastics demand, with a market share of 34.4% for polyethylene (PE) and 24.2% for polypropylene (PP) [2]. PE and PP, whose chemical formulas are presented in Fig. 1, are produced mainly from oil and natural gas via a polymerisation process of ethylene or propylene, respectively. The versatility of their synthesis enables the fabrication of different grades, covering a wide range of beneficial properties. Low density polyethylene (LDPE) presents the most extensive degree of branching among polyolefins, and a degree of crystallinity which typically varies between 40–55%. As a result, it is easy to process

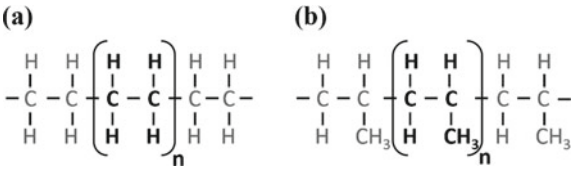

Fig. 1 Chemical structure of **a** polyethylene and **b** polypropylene. The structure presented for the latter represents its isotactic configuration, with the methyl group always on the same side of the main chain

and is not reactive at room temperature, making it suitable for use in reusable bags and food packaging films. Because of its very reduced amount of branching, crystallinity in high density polyethylene (HDPE) can reach 70–80%, resulting in higher tensile strength and thermal resistance than LDPE. HDPE is used in toys, milk, or shampoo bottles. Ultra-high molecular weight polyethylene (UHMWPE) is characterized by its extremely long chains, reaching molecular weights in the order of 10^6 g/mol. It embodies the advantages of HDPE and it has great chemical resistance, as well as having the best impact strength among thermoplastics. These properties make UHMWPE an excellent material for personal armor and medical implants. PP generally presents better mechanical properties and thermal resistance than PE, but its chemical resistance is lower. The most widely used is isotactic PP (i-PP), in which the methyl group is on the same side of the main chain (Fig. 1b), with a crystallinity in between that of LDPE and HDPE. PP is widely used in food packaging, bank notes, and sweet or snack wrappers.

In most of these products, the fundamental understanding of the relationship between the internal structure and dynamics of the polymer and the final properties are key to optimize performance. One of the most valuable techniques to obtain such understanding at a molecular and chain level is dielectric spectroscopy, which measures the relaxation of dipoles present in the material after the application of an external electric field of varying frequency [3]. This technique relies on the presence of polar molecules, whose orientation can be affected by the external field and their reorientation back to equilibrium can be detected. However, the chemical structure of polyolefins is nonpolar, resulting in a lack of dipoles which renders them dielectrically inactive in the absence of impurities. Different approaches have been studied to introduce dipoles in polyolefins, involving either chemical modifications to introduce polar groups such as direct oxidization, chlorination, or indirect oxidization through the introduction of inorganic fillers, as well as the addition of probes with a large permanent dipole moment. In this chapter, we will first discuss representative dielectric spectra of the most common variations of PE and PP, followed by a discussion on the different approaches used to render them dielectrically active. Then, we will present a summary of the studies on polyolefin composites for electrical energy storage and insulation applications.

2 Dielectric Spectra Overview

Dielectric relaxation dynamics of PE and i-PP have been extensively studied for decades, either relying on the presence of dipoles originated by impurities or sample preparation, or actively introducing dipoles in the polymer by different methods which will be reviewed in the following section. In this section, as a background for the rest of the chapter, we will give an overview of the different relaxations found in the different grades of PE and i-PP, as well as the current knowledge on their molecular origins.

Representative dielectric spectra for LDPE, HDPE, and i-PP are shown in Fig. 2. Both PE and i-PP (Fig. 2a-c) display three characteristic relaxations, traditionally named α, β, and γ, in order of decreasing temperature, with a fourth process at very low temperatures, δ, which is weak or absent in some cases. The α relaxation, associated to the crystalline phase, is attributed in PE to the longitudinal motion of polymer chains through the crystalline lamellae, in a helicoidal movement [4, 5]. As a result, the α relaxation is much more intense in HDPE when compared to LDPE, as the former has a higher degree of crystallinity and more chains in the crystalline phase to contribute to this process. The origin of the α process in i-PP is still a topic of debate, with evidence from mechanical experiments that it is due to a relaxation of defects in the crystalline phase with some additional contribution from the neighboring

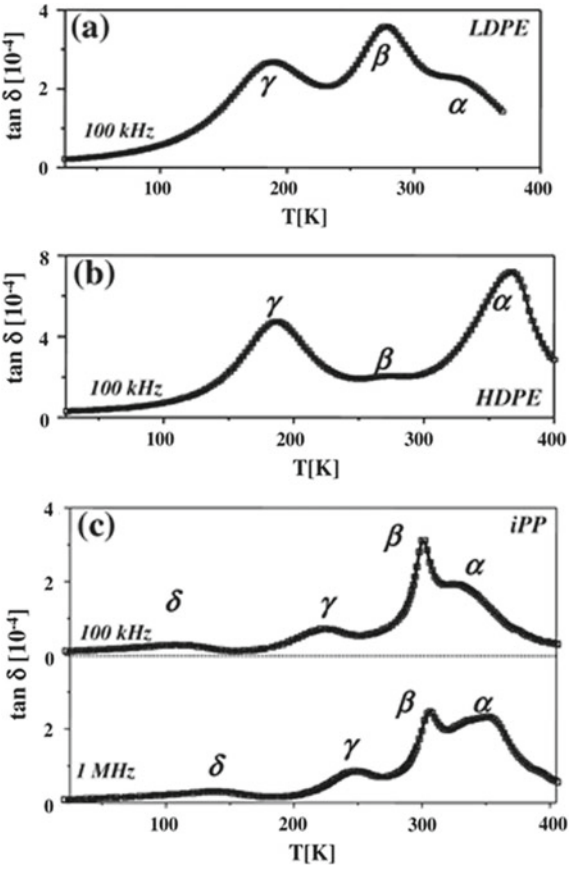

Fig. 2 Dielectric loss tangent for semicrystalline polyolefins as a function of temperature: **a** low density polyethylene (LDPE). **b** high density polyethylene (HDPE), and **c** isotactic polypropylene (iPP). Adapted with permission from Milicevic, D. Et al. Radiation-Induced Modification of Dielectric Relaxation Spectra of Polyolefins: Polyethylenes vs. Polypropylene. *Polym. Bull.* **2014**, *71*, 2317–2334

amorphous regions [6]. Dielectric [7] and mechanical [8] studies prove that the α process in i-PP is multicomponent, involving two or three subprocesses. The next process in order of increasing temperature is the β relaxation, which is related to the glass transition in both PE [9] and i-PP [6]. This process is more intense in LDPE than in HDPE, as the crystallinity is lower for LDPE and there are more amorphous chains available to contribute to the glass transition. Then we have the γ relaxation, which in PE is assigned to the movement of certain parts of chains in the amorphous regions in the vicinity of the crystalline lamellae. Several γ subprocesses have been reported, but their assignment to specific molecular dynamics is not fully clear yet [10–12]. In i-PP, the γ process has been related to the movement of chain ends or branches, in a crankshaft-type fashion, in mechanical and dielectric studies [8, 13, 14]. A fourth relaxation has been reported at very low temperatures in both PE and i-PP, the δ process. This relaxation has been correlated with hindered rotation of CH_3 groups [14, 15] and it is generally weak or absent. It is expected to be especially weak in the case of PE, where the CH_3 groups can only be found at the chain ends.

We believe it is of importance to mention that the matter of polyethylene's glass to rubber transition temperature has been an ongoing matter for decades and some researchers still do not fully agree on its assignment. Various works over the years have proposed that either the β-relaxation [16, 17] or the γ-relaxation [18, 19] correspond to the dynamic glass to rubber transition process. It has even been suggested that polyethylene has two glass transitions, γ-relaxation for linear polyethylene and β-relaxation for branched polyethylene [20, 21]. Generally, in semicrystalline polymers, the β-relaxation appears to be broadened when compared with amorphous samples and considerably less prominent than the β-relaxation, supporting the idea that the β-relaxation is the dynamic glass to rubber transition process [16]. On the other hand, the γ-relaxation has been found to increase in intensity with decreasing crystallinity, and has been assigned to mobile groups of amorphous chains in the vicinity of crystalline lamellae [22, 23]. For these reasons, and as described before, here we will follow the most widespread approach in the community of assigning the β relaxation to the glass transition of PE and the γ relaxation to a process associated to movement of localized amorphous chain segments.

3 Methods to Introduce Polar Groups

The unveiling of the dielectric spectra of polyolefins, whose nonpolar structures result in the absence of a permanent dipole moment, has only been possible thanks to the introduction of dipoles. For the polymer to be dielectrically active and enable the measurement of its relaxation spectra, such introduction of dipoles must have taken place, either unintentionally (e.g. oxidization due to impurities or sample preparation conditions) or intentionally. We will now review the different methods used to render PE and i-PP dielectrically active, as well as the influence these procedures have on their final dielectric spectra. Methods are classified into two types: (i) those that rely

on the chemical modification of the polymer chain to induce dipoles and (ii) the addition of probes with strong dipole moment into the polymer matrix.

3.1 Chemical Modifications

We will first report on methods that render polyolefins dielectrically active by means of chemical modifications, including oxidization and chlorination. The most common is oxidization, which introduces carbonyl groups into the polymer chain that serve as a dielectric probe. Thermally-initiated oxidization was one of the first methods to be used, which enabled the unveiling of the dielectric spectra of PE early on [24–26]. Boyd argued that the α relaxation observed in lightly oxidized PE must involve the screw rotation around the main chain axis of a perpendicular C=O dipole which is yielding the necessary dielectric activity to detect the process [4, 16]. Several studies have reported on the use of gamma radiation to oxidize PE and i-PP [12, 27–29]. As shown in Fig. 3, the dielectric losses of some relaxations increase with increasing doses, but after irradiation, some of the processes are not present anymore. For example, the disappearance of the β relaxation in HDPE and i-PP upon irradiation has been attributed to an increase in crystallinity due to chain scission and the occurrence of crosslinking, which reduces chain mobility [12, 27, 28]. The disappearance after irradiation of the γ process has been associated in mechanical measurements to the increase in carbonyl content and the decreased molecular weight of the highly oxidized PP due to chain scission [30, 31].

Artificial weathering has been proposed as an alternative to thermal oxidation, using UV radiation in a dry environment to induce photo oxidative chain scission

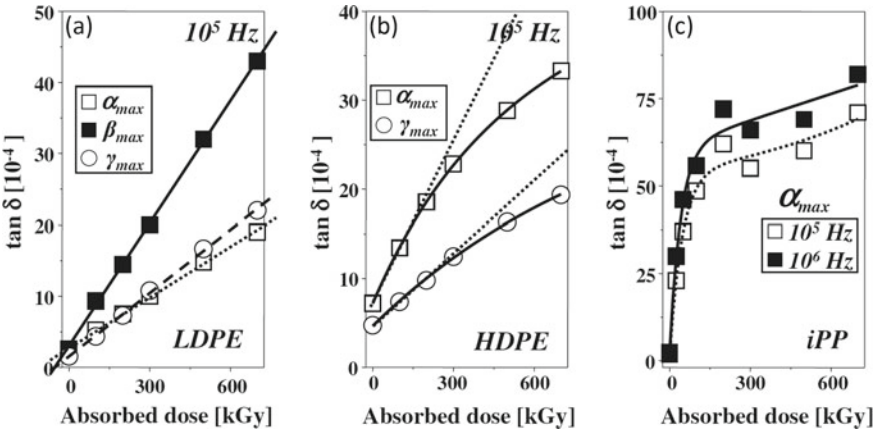

Fig. 3 Dielectric loss tangent versus absorbed dose for **a** LDPE, **b** HDPE, and **c** i-PP. Reproduced from Radiation-Induced Modification of Dielectric Relaxation Spectra of Polyolefins: Polyethylenes versus Polypropylene . *Polym. Bull.* **2014**, *71*, 2317–2334, reproduced with permission

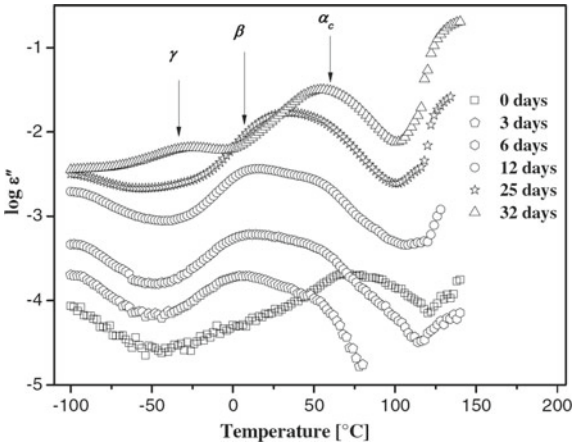

Fig. 4 Dielectric loss ε" versus. temperature of UV-weathered PE at a frequency of 1000 Hz for 0 (square), 3 (pentagon), 6 (hexagon), 12 (circle), 25 (star), and 32 (triangle) days of weathering. The three relaxation processes, namely α, β, and γ appear in order of decreasing temperature. The α relaxation is observed only for 25 (star) and 32 days (triangle) weathered LDPE in the given temperature range. Reproduced with permission from Ramanujam et al. [32]

in LDPE followed by cross-linking [32]. As weathering time increases, a balance is achieved between an increase of the glass transition temperature due to cross-linking and further crystallization of newly created shorter polymer chains, and a decrease of T_g related to the increase in free volume that the dangling chain ends provide. As shown in Fig. 4, the unirradiated sample presents a weak dielectric response, whereas the UV-weathered samples show an increasing dielectric strength as weathering time increases, until at 32 days all relaxations (α, β, and γ) are visible in the spectra. However, for these long weathering times, the polymer films were very brittle, leading to the complete loss of structural integrity.

Chlorination, consisting in the introduction of chlorine atoms as a side chain group, has been proven successful as well in rendering polyethylene dielectrically active. It has been reported that the dielectric strength of the α relaxation in chlorinated polyethylene is not proportional to its crystallinity, [24] as the chlorine atoms favor the amorphous phase [33].

In some cases, the introduction of inorganic fillers in a polymer matrix can result in chemical modifications that generate dipoles in the chain. Metal oxide nanomaterials can oxidize the polymer chains and generate the carbonyl groups needed to increase the number of dipoles present. Frübing et al. introduced different contents of titanium dioxide (TiO_2) nanoparticles (200 nm in diameter) in LDPE, enabling them to observe the α, β, and γ relaxations [9]. Figure 5 shows the relaxation map of LDPE with different TiO_2 contents. The relaxation map shows that with increasing TiO_2 content, the β process shifts to higher temperature values. This is because the TiO_2 particles tend to remain in the amorphous phase, rendering it more rigid and hindering chain movement. On the other hand, the position and slope of the Arrhenius plots of the

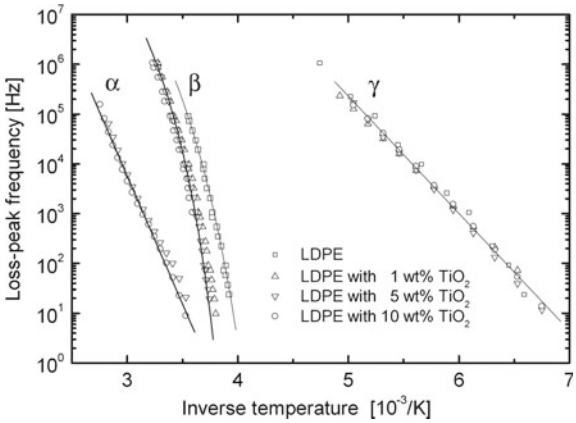

Fig. 5 Relaxation maps of LDPE with different titanium-dioxide content as indicated. The full curves are Arrhenius fits to the α and γ relaxations of LDPE with 10 wt% TiO_2 as well as VFT fits to the β relaxation of LDPE and LDPE with 5 wt% TiO_2. Reproduced with permission from Frübing et al. [9]

α and γ relaxation are hardly changed by the addition of TiO_2. In this case, if the filler remains in the amorphous phase, it is not expected to affect a crystalline phase process (α) and it will only influence a localized process (γ) if it is close to it, which for a low TiO_2 content it is unlikely. The authors reported that the dielectric strength of the α relaxation increases with increasing TiO_2 content and attributed this to the increased presence of carbonyl groups formed in the melt during sample preparation.

We recently studied the dielectric behavior of disentangled UHMWPE, [10] which contains a much lower fraction of entanglements than the commercial UHMWPE. The use of methylaluminoxane (MAO) as a catalyst in the polymerization reaction results in the presence of aluminum oxide (Al_2O_3) traces which oxidize the polymer chain and create carbonyl groups in the chain that renders the polymer dielectrically active [34, 35]. The disentangled character of our UHMWPE results into a non-equilibrium melt-state leading into an increase in elastic shear modulus G' in time due to the progressive formation of entanglements [36]. The plateau modulus at thermodynamic equilibrium, G_N^0, can be calculated as [37]:

$$G_N^0 = \frac{g_N \rho RT}{M_e} \tag{1}$$

where g_N is a numerical factor, r is the density of the material at the absolute temperature T, R is the gas constant. M_e is the molecular weight between entanglements, and it is inversely proportional to the entanglement density.

To follow the entanglement process in the melt state, dielectric spectra of UHMWPE during consecutive frequency sweeps were acquired at a constant temperature of 160 °C, considerably above the melting point of the material which is around

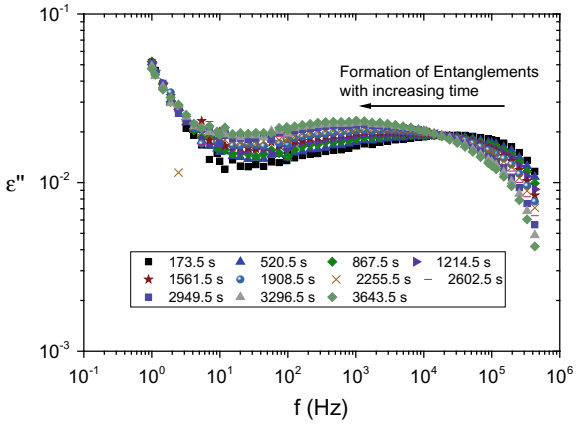

Fig. 6 Imaginary part of dielectric permittivity ε″in disentangled UHMWPE during consecutive frequency sweeps at a constant temperature of 160 °C. The shift toward lower frequencies is indicative of entanglement formation and reduced chain mobility. Adapted (Creative commons license) from Drakopoulos et al. **150**, 35 [10]

140 °C. As presented in Fig. 6, the main dielectric signal shifts toward lower frequencies as entanglements form over time and the chain mobility is hindered [38]. In order to try to establish a correlation with the elastic shear modulus *G* from rheology, the complex electric modulus *M** was calculated as follows:

$$M^* = \frac{1}{\varepsilon^*} = \frac{1}{\varepsilon' - i\varepsilon''} = \frac{\varepsilon'}{\varepsilon'^2 + \varepsilon''^2} + \mathrm{i}\frac{\varepsilon''}{\varepsilon'^2 + \varepsilon''^2} = \mathrm{M}' + i\mathrm{M}'' \tag{2}$$

where *M'*, and *M"* are the real and the imaginary parts of the electric modulus, respectively, *ε** is the complex permittivity and *ε'* and *ε"* are the corresponding real and imaginary parts, in analogy to the complex modulus defined for other types of dynamic measurements. Figure 7 shows graphs for M' as a function of time at 160 °C, showing how the electric modulus, which is the inverse of permittivity, increases in time reaching a plateau. The same behavior can be observed for the elastic shear modulus obtained by rheology. The formed entanglements restrict the motion of filler-induced polar groups hindering their ability to align with the electric field. Consequently, polarization and permittivity diminish approaching a constant value as entanglements are formed.

3.2 Introduction of Dielectric Probes

As presented in the previous section, chemical modifications to introduce polar groups in the polymer chain can lead to undesired consequences such as changes

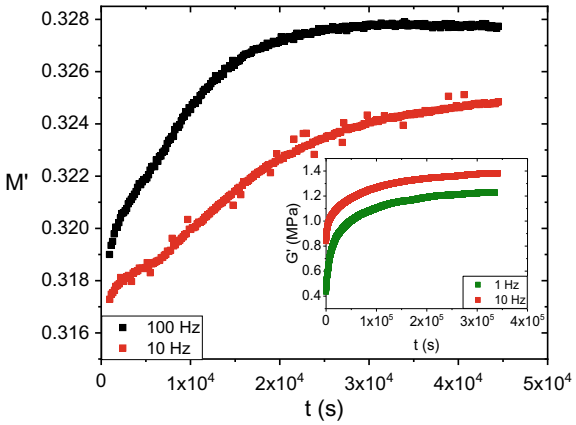

Fig. 7 The real part of electric modulus for disentangled UHMWPE at 160 °C as a function of time at 10–100 Hz. The inset shows elastic shear modulus as determined by rheology at 1–10 Hz. Adapted (Creative commons license) from Drakopoulos et al. **150**, 35 [10]

in crystallinity, [33] chain scission [31], and crosslinking [32]. Therefore, the introduction of small molecules that, rather than inducing dipoles in the polymer, carry their own permanent dipole moment, has been explored in recent years as a less invasive alternative.

Van den Berg et al. [39] introduced a 4,4-(N,N-di- butylamino)-(E)-nitrostilbene (DBANS), which has a large dipole moment (9D), in LDPE and i-PP at low concentrations (up to 1 wt%) to aid the measurement of their dielectric spectra. DBANS is a rigid rod-like molecule, eliminating possible signals coming from relaxations associated with intramolecular motions, and does not tend to crystallize due to its butyl tails. The dielectric loss ε" versus temperature graphs of LDPE and i-PP doped with different concentrations of DBANs are shown in Fig. 8. For undoped LDPE (Fig. 8a), the three main relaxation processes are observed, α, β, and γ. This is an indication of the occurrence of oxidation of the polymer possibly due to the presence of impurities. However, the dielectric losses are very low, in the range of 10^{-4}-10^{-3}. After the addition of DBANS, clear changes are observed in the dielectric spectra of LDPE, the most evident being a significant enhancement of the strength of the β relaxation. The probe does not seem to enhance the crystalline α relaxation, which is expected as the small molecules are more likely to dissolve in the amorphous phase. Moreover, the small concentrations of DBANS used minimizes the chances of influencing the strength of localized processes such as the γ relaxation, which remains fairly unaltered. The fact that the probe only enhances the β relaxation, attributed to the glass transition, implies that the DBANS molecules feel the changes in local viscosity associated with this process without the influence of other local phenomena. A similar effect is observed when DBANS is added to i-PP, as shown in Fig. 8b, where mainly a strengthening of the glass transition process (β) is observed. For both PE and i-PP, it was found that the dielectric enhancement of the dielectric

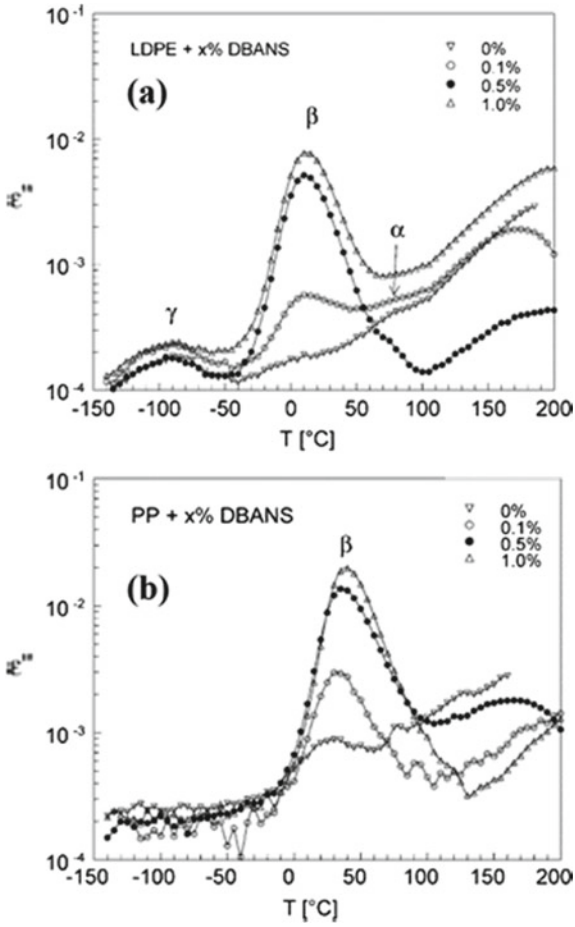

Fig. 8 Dielectric loss ε''(T) at f = 13 kHz for **a** undoped LDPE and three LDPE/DBANS blends, and **b** undoped i-PP and three i-PP/DBANS blends. Reprinted with permission from Van Den Berg et al. [39]. Copyright 2004 American Chemical Society

glass transition process is proportional to the probe concentration up to about 0.5 DBANS wt %, and that the relaxation time remained within one order of magnitude in frequency of that of the pristine polymer.

The same probe has been introduced in blends of PP and LDPE to study the glass transition dynamics [40]. PE-PP blends with different compositions and morphologies presented substantially the same glass transition dynamics, indicating a bulk behavior for both components. One of the main concerns when adding a dielectric probe to a polymer blend is the preference of the probe to migrate to one of the components or the blend or the interface between the different fractions, resulting in a dielectric signal which does not represent the blend system accurately. In this study, the relaxation strength normalized by the weight fraction of each polymer stayed constant for all compositions. Therefore, the distribution of the dielectric probe was homogeneous across the different phases of the sample.

4 Polyolefin Composites for Electrical Energy Storage and Insulation

4.1 Background

In recent years, renewed effort has been invested in the investigation of the storage, efficient recovery and distribution of electrical energy, affecting directly an interdisciplinary range of scientific fields, from fundamental and applied natural sciences to economics and sociology. The need for new advancements in the energy materials goes in parallel with the drawbacks of oil as a source of fuel, such as its impact on climate change and variable cost. In addition, other sources of electrochemical energy such as batteries are characterized by long recharging hours, thus limiting the applicability for future fast-responsive applications, [41] and technologies that are hazardous for the environment, generating a demand for more effective and safer storage materials.

Insulating materials used as dielectric mediums to store capacitive electrical energy find application in many modern electronic systems, ranging from electronic devices to hybrid electric cars [42]. For such applications, a specific combination of properties is required including [43–46]: (i) High values of dielectric permittivity, which is a measure of the ability of the material to store energy; (ii) low dielectric loss (tanδ) values, to maximize efficiency; (iii) low electrical conductivity, in order to reduce leakage currents; and (iv) high dielectric breakdown strength so higher electrical fields can be physically endured by the dielectric medium. Polymers, and especially non-polar ones such as polyolefins, are characterized by low values of dielectric permittivity and high breakdown strengths. In contrast, ceramic materials exhibit the exact reciprocal behavior, presenting high permittivity and low breakdown strength. Therefore, composite materials composed of a polymer matrix and ceramic nanofillers are a priori great candidates for electrical energy storage materials [47].

In heterogeneous dielectric nanomaterials, understanding the role of interface/interphase properties and the possibility to tailor them at will is of great scientific and technological importance [48, 49]. In this respect, semicrystalline polymers often are considered as heterogeneous materials, with the amorphous regions of the polymer chains forming the continuous matrix phase and the rigid crystallites in the role of the filler [50]. The crystallinity and crystal morphology also affect the dielectric properties by enhancing interfacial polarization phenomena [51], and increase the dielectric breakdown strength due to higher resistance to electrical treeing (current propagation to failure) [52]. Toward this direction, biaxial orientation of semicrystalline polymers, like polypropylene, has found use as thin dielectric membranes for electrical energy storage applications [53]. In addition, fillers of various shapes, electrical characteristics and orientation, have been employed to enhance the dielectric behavior of such polymers [43].

The addition of electrically conducting fillers within an insulating polymer matrix can enhance their electrical and electromagnetic properties for applications in electromagnetic interference shielding and conductive adhesives in circuit elements in the

microelectronics industry [54]. Due to the vastly different electrical conductivities between the constituents of such system, the direct-current conductivity is strongly dependent on the conducting filler concentration, thus leading to two basic charge transport mechanisms:

(i) At low filler concentrations, the mean distance between conducting fillers is sufficiently high and so the electrical properties of the composite are dominated by the insulating matrix. In such cases, the charge carriers (in most cases electrons, ions, and holes) hop to a nearby state that can be quantum-mechanically described with higher or lower energetic jumps of the potential barrier, the latter achieved through quantum tunnelling [55].
(ii) At concentrations equal or higher than the percolation threshold, the conducting fillers are in contact and the charge carriers can move with low resistance (current flow), exhibiting the behavior of a conductor [56]. This can also be determined by the temperature dependence of electrical conductivity. In dielectric materials, conductivity increases with temperature due to higher mobility of charge carriers, whereas in conductors conductivity decreases with temperature due to polaron scattering effects [57].

The movement of the charge carriers from the conductive fillers can cause a dipolar response from the insulating polymer matrix and the corresponding interphase as well, leading to a Maxwell–Wagner–Sillars interfacial polarization and increasing the capacitive storage ability of the resulting composite [58]. Surface modification processes to customize the interfaces between the matrix and the filler have been extensively studied in the past decade to enhance dielectric performance. These modifications affect the polarizability of the polyolefin matrix by introducing polar groups and enhancing the hydrophobicity, resulting into better-performing insulating materials [59].

4.2 Polyethylene Composites

Polyethylene is traditionally employed as an insulating material for cable manufacturing, due to its extremely weak conductivity and high dielectric breakdown strength. The two are interconnected, as the dielectric breakdown strength is dependent on electrical conductivity; the addition of high permittivity or high conductivity particles will enhance or decrease the dielectric breakdown strength, respectively. Moreover, the presence of agglomerates forming a percolating network can highly improve the thermal conductivity of the nanocomposite but decrease the dielectric breakdown strength [60]. In polyethylene/montmorillonite composites, Li et al. observed that the inclusion of aligned fillers results in an enhancement of the dielectric breakdown response that adds up to that provided by the oriented polymer crystals [61]. This effect could be exploited in materials that already present a drastic improvement of thermal conductivity when stretched, such as UHMWPE, [62] to provide a suitable material for electrical energy storage.

Another very important factor for cable insulation applications is the desired hydrophobic character of the dielectrics in use; the unwanted water molecules induce charge transport resulting into poor dielectric breakdown strengths and failure. Studies of hydrophilic/hydrophobic nanofillers at different humidity environments have shown that the drawbacks from the moisture sorption can be greater than the benefit of having the ceramic nanofiller in some cases [63]. As it can be observed in Table 1, composites with oxide fillers perform much worse in ambient and wet environments when compared with dry conditions, whereas composites using nitride fillers had a much more consistent response under ambient humidity. *Ayoob* et al. introduced hexagonal boron nitride in polyethylene to impart good great thermal conductivity and hydrophobicity to the polymer matrix, resulting in minimal charge transport at even very high filler concentrations (30% w/w) [60]. To reduce the drawbacks from the diffusion and adsorption of water molecules intended for such applications, chemical modification of the surface between the fillers and the polymer matrix can be implemented [64].

Other key features to consider when designing new composite insulators are the geometry and orientation of the fillers. Montmorillonite (MMT) nanosheets characterized by a high aspect ratio, have been proved to diminish the electrical treeing, through the encapsulation of mobile charge carriers in the interfaces between the matrix and the nanosheets [43, 49]. Further enhancement on the dielectric properties was observed by inducing filler orientation, which yields higher dielectric breakdown strength and higher energy efficiency when compared to an isotropic system of the same composition [43]. The anisotropic character can be enhanced further by orienting the crystalline and amorphous domains of the polymer matrix

Table 1 DC breakdown values for polyethylene composites with oxide and nitride fillers in different humidity environments [63]. Adapted from Hosier et al. The effects of hydration on the DC breakdown strength of polyethylene composites employing oxide and nitride fillers. IEEE Transactions on Dielectrics and Electrical Insulation 2017, 24, 3073–3082

Nominal filler content and type	Ambient conditioning (MV/m)	Dry conditioning (MV/m)	Wet conditioning MV/m
–	416 ± 30	425 ± 32	408 ± 32
5 wt. % Si_3N_4	409 ± 30	431 ± 34	172 ± 14
10 wt. % Si_3N_4	389 ± 30	450 ± 27	150 ± 12
5 wt. % SiO_2	228 ± 14	431 ± 30	135 ± 12
10 wt. % SiO_2	194 ± 12	414 ± 30	102 ± 7
5 wt. % AlN	366 ± 19	362 ± 18	241 ± 14
10 wt. % AlN	362 ± 18	373 ± 15	350 ± 26
5 wt. % Al_2O_3	349 ± 17	393 ± 24	241 ± 14
10 wt. % Al_2O_3	259 ± 15	360 ± 25	154 ± 12
5 wt. % SiO_2©	425 ± 42	442 ± 34	295 ± 26
10 wt. % SiO_2©	463 ± 29	436 ± 20	207 ± 23

by melt-state or solid-state processing, resulting in an improvement of the electrical breakdown properties. As it can be observed in Fig. 9, the breakdown strength of polyethylene/organo-montmorillonite (o-MMT) composites increases as they are stretched further [65]. A percolative behavior of normalized breakdown strength with crystalline orientation (strain) can be seen in Fig. 9b for PE composites with 9 wt% of o-MMT. The observed increase in breakdown strength was correlated with crystal orientation, as the crystallites provide higher potential barriers for electrical treeing [66].

The introduction of conducting fillers can impart to highly insulating polyethylene semiconducting electrical behavior even at low filler concentrations. The effect of such fillers in polyethylene in DC (s_{dc}) and AC (s_{ac}) conductivities can be appreciated in Figs. 10 and 11 where carbon nanofibers (CNF) or multi-wall carbon nanotubes

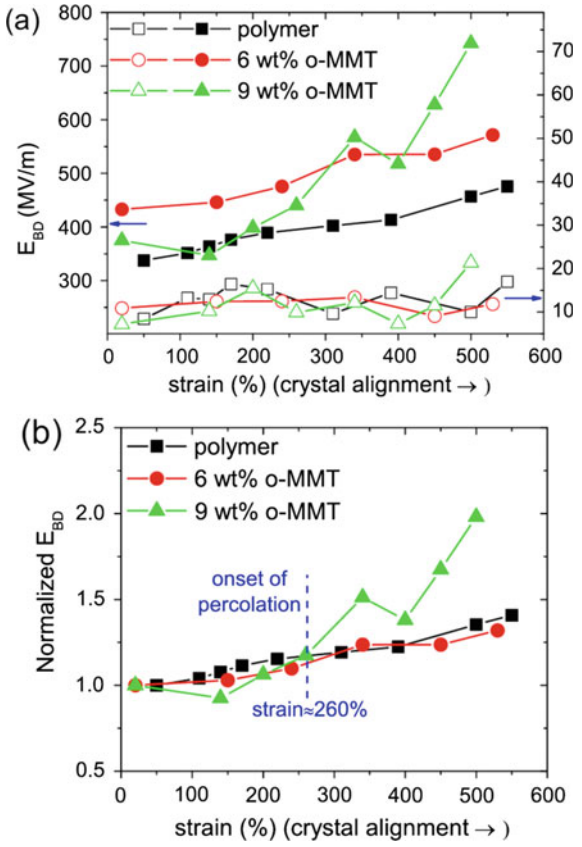

Fig. 9 Electric breakdown properties of polyethylene nanocomposites with different contents of organo-montmorillonite as a function of strain: **a** Weibull breakdown strength (E_{BD}) and Weibull modulus (b_w) and **b** normalized E_{BD} with respect to the first low-strain breakdown point in each film [65]. Reproduced with permission from Li et al. Appl. Phys. Lett. 111, 082,906 (2017)

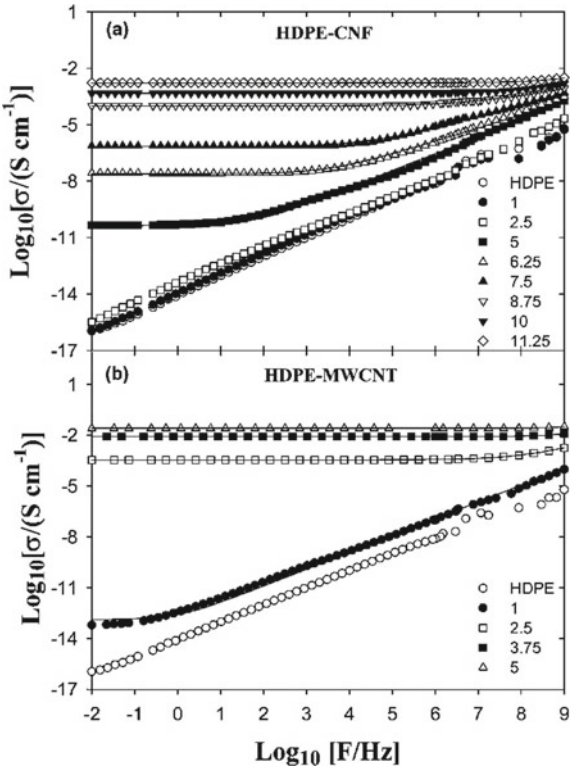

Fig. 10 AC conductivity as a function of frequency for HDPE composites with **a** carbon nanofibers (CNFs) and **b** Multi-wall carbon nanotubes (MWCNTs) for different filler concentrations [67]. Reproduced with permission from Linares et al. Macromolecules 2008, 41, 7090–7097

(MWCNT) are added to high density polyethylene (HDPE). In Fig. 10, it can also be appreciated that with the increase of fillers concentration, the AC conductivity becomes increasingly less dependent on frequency [67]. Since there is a contribution of DC conductivity to the imaginary part of dielectric permittivity $\left(\frac{\sigma_{dc}}{\omega\varepsilon_0}\right)$ when the s_{dc} becomes sufficiently high, it shadows the molecular dipolar response originating from the dielectric material resulting into $s_{ac}(f,T) \approx s_{dc}(T)$. This effect is considerably more intense in polyolefins such as polyethylene due to their very weak relaxation strengths ($\Delta\varepsilon = \varepsilon_s - \varepsilon_\infty$).

As it can be appreciated from Fig. 11, the percolation threshold of CNF and MWCNT in DC current is found to be at 3 and 1% v/v, respectively, which according to percolation theory, is the concentration where a continuous network of conductive fillers is formed. It is significant to note that the electrical conductivity of the nanocomposites at the percolation threshold is around 14 orders of magnitude the one of plain polyethylene, highlighting the enhancement of the electrical properties.

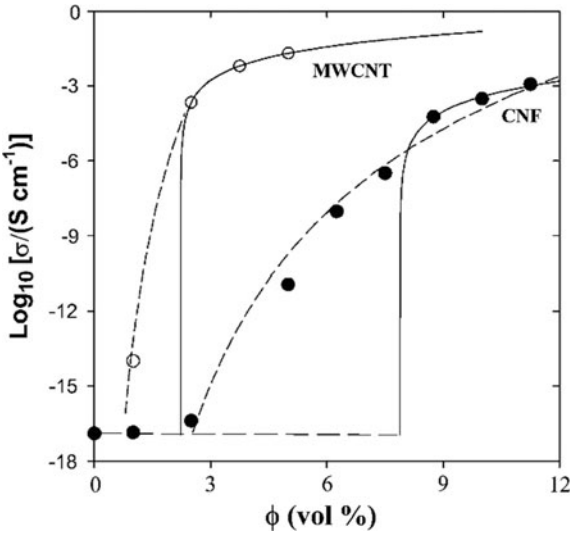

Fig. 11 DC conductivity as a function of filler volume concentration of polyethylene nanocomposites with carbon nanofibers (CNF, solid symbols) or multi-wall carbon nanotubes (MWCNTs, empty symbols) [67]. Reproduced with permission from Linares et al. Macromolecules 2008, 41, 7090–7097

4.3 Polypropylene Composites

Polypropylene is currently the material of choice for capacitor applications over several other polymers (e.g., polystyrene, polyethylene terephthalate) due to its very low dissipation factor ($tan\delta < 0.001$), superior dielectric strength (~700 MV/m), thermal stability (130 °C < T_m < 170 °C), and its easier melt processing [53, 68]. Advancements in the chemistry of polyolefins has resulted into isotactic polypropylene (iPP) exhibiting an isotacticity of 97–99% and very low impurity concentration (30 ppm), facilitating processing and bringing its melting point of around 165 °C [69]. In industrial settings, the financial aspects related to the manufacturing conditions play a significant role on the choice of material. For the aforementioned reasons, polypropylene has remained the best option for over half a century. Since 1963 and the MAGVAR invention from General Electric, biaxially oriented polypropylene films have been employed in capacitor applications, as they provide a thin and efficient energy solution for the storage and recovery of electrical energy [68]. The orientation in these films can be achieved through several methods, including simultaneous stretching in two perpendicular directions utilizing an apparatus such as the one presented in Fig. 12. However, in industry, the prevalent approach is the tubular process, which enables continuous production of BOPP [70].

During the earliest tests on unoriented polypropylene, it became clear that orientation is paramount to achieve time endurance, as an increase in dielectric breakdown strength by at least a factor of 2 is achieved with the orientation process. Nash

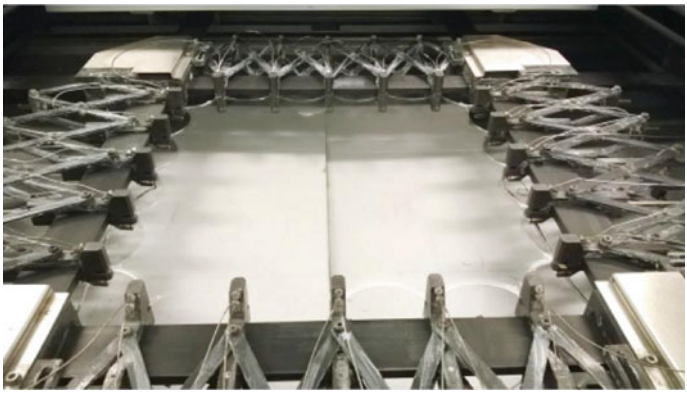

Fig. 12 A biaxial stretching machine [53]. Reproduced with permission from Ryroluoto et al. European Polymer Journal, 2017, 95, 606–624

performed a thorough comparison (averaging 70 production samples) between the dielectric breakdown strength values of oriented and unoriented polypropylene films [68]. The enhancement in the dielectric breakdown strength upon orientation, shown in Fig. 13, is attributed to the transformation of the spherulitic crystalline morphology to a highly ordered fibrillar network, consisting of oriented crystallites [53]. As in the case of polyethylene composites, the improvement of the dielectric breakdown

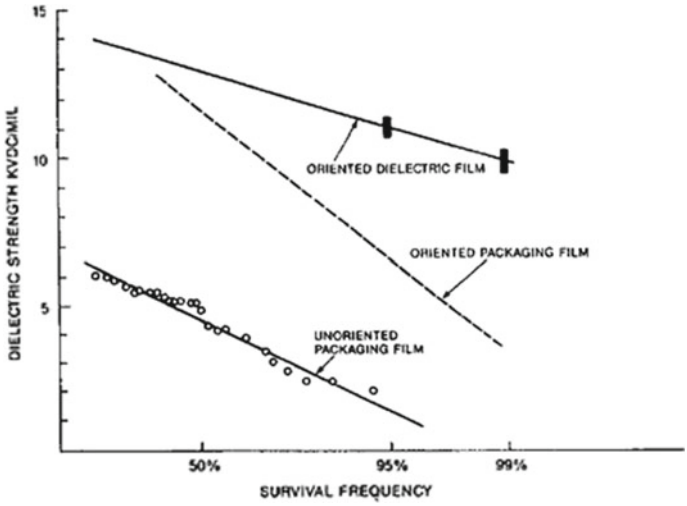

Fig. 13 Dielectric breakdown strength of unoriented and biaxially oriented polypropylene packaging films [68]. J.L Nash, Polymer Engineering and Science, 1988, 28, 862–870. Reproduced with permission

strength due to orientation can be attributed to the crystallites acting as a barrier against treeing [66].

Two more parameters have been found to play a significant role on the dielectric properties of biaxially oriented polypropylene. The first factor is that with orientation, the porosity decreases enhancing thus the dielectric breakdown strength. This is explained on the basis that the density of the material increases through the alignment of the amorphous segments and crystallites [53]. Therefore, orientation reduces the topological electric field enhancement generated around microcavities that induces dielectric failure and breakdown. The second factor relies on the crystal transformation of polypropylene from the β to the α crystal phase that takes place upon stretching. An inversely proportional relationship has been found between the amount of β-phase and the dielectric breakdown strength which also connects with the presence of microvoids within the sample [53]. As shown in Fig. 14, the dielectric breakdown strength is reduced when the β-phase content is increased, thus predicting a better dielectric stability for oriented samples.

Different nanosized inorganic fillers have been used to dope polypropylene and enhance its dielectric properties, resulting in the development of the so-called nanodielectric materials. Calcium carbonate ($CaCO_3$) particles, which are highly polar, are often employed as fillers due to their low commercial price and good thermal resistance. When their size is in the nanoscale (1–100 nm), their inclusion in a propylene matrix increases the dielectric direct-current breakdown, which reaches a maximum at 1.8 wt.% concentration [71]. However, they tend to agglomerate and are hydrophilic, which can be detrimental for electrical energy storage applications [72]. These drawbacks can be avoided through surface modification and chemical functionalization, which can reduce hydrophilicity of the particles and improve the

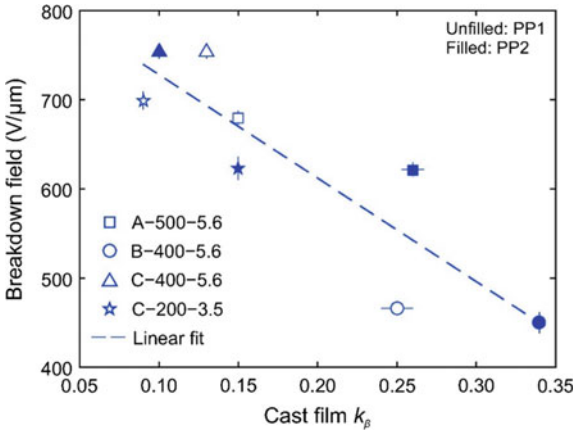

Fig. 14 Breakdown field as a function of the β crystal phase content in two isotactic polypropylenes PP1 and PP2, with Mw, PDI, Tm to be equal to 400 kg/mol, 6.0, 161 °C, and 300 kg/mol, 8.0, 163 °C, respectively [53]. Reproduced with permission from Ryroluoto et al. European Polymer Journal, 2017, 95, 606–624

Table 2 Dielectric properties of metal-isotactic polypropylene nano-composites having different volume fractions of Al nanoparticles in the polymer matrix [75]. Adapted from Fredin et al. Substantial recoverable energy storage in percolative metallic aluminum-polypropylene nanocomposites. Advanced Functional Materials 2013, 23, 3560–3569

Al particle vol%	Permittivity	Interparticle distance (nm)	Dielectric breakdown strength (MV/m)	Al particle vol%
0.7	2.4 ± 0.4	321.3	123.7	0.7
2.0	2.8 ± 0.9	196.9	–	2.0
2.9	3.0 ± 0.4	162.3	85.2	2.9
10.4	10.5 ± 0.3	71.4	119.3	10.4
12.4	15.4 ± 0.1	61.6	75.8	12.4
25.4	conductive	27.3	–	25.4
38.2	conductive	11.1	–	38.2
40.8	conductive	8.7	–	40.8

adhesion/compatibility. The latter effect can enhance the mechanical properties, such as the case when stearic acid is used as a functionalization agent [73]. Another range of ceramic nanoparticles that improve the dielectric behavior of polypropylene are those of very high dielectric constants, like barium titanate (BaTiO3, $\varepsilon_r \sim 2{,}000$). It has been proven that the addition of the $BaTiO_3$ nanoparticles combined with uniaxial orientation can indeed result in high energy densities [74].

Besides ceramic nanofillers, metallic nano-inclusions can be added to enhance the interfacial polarization and hence the dielectric constant of the resulting composite. Table 2 and Fig. 15 show the permittivity and dielectric breakdown strength values for polypropylene composites with metallic aluminum nanoparticles. The composite's permittivity increases up to $\varepsilon_r = 15.4$ for a volume fraction of nanoparticles of 12.4%. This maximum permittivity is reached just before the percolation volume fraction, 16%.

5 Conclusions

In this chapter, we have elaborated on the importance of understanding the correlations between structure, molecular dynamics, and properties in polyolefins and their composites, and how to overcome the difficulties of obtaining insights from dielectric spectroscopy in such nonpolar polymers. We can draw three main conclusions:

1. Different approaches have been successfully implemented to render polyolefins dielectrically active through the introduction of permanent dipoles in the system. These methods might take place either inadvertently during sample preparation/synthesis or deliberately, and include the following: Direct oxidization through thermal treatments, UV-weathering, or gamma radiation exposure, to introduce carbonyl groups in the polymer chain; indirect oxidization, induced by

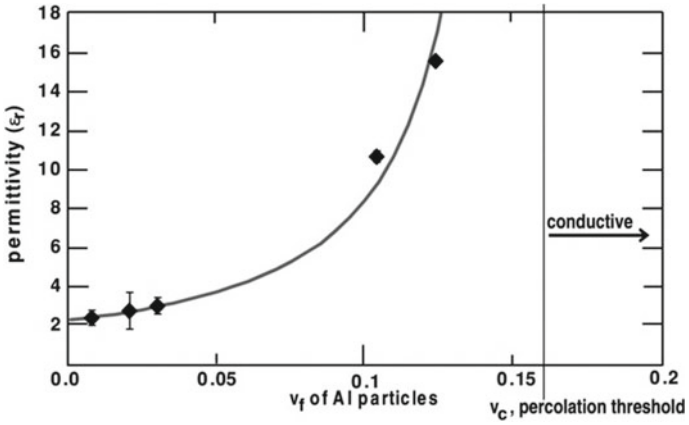

Fig. 15 Experimental permittivity for Al– iso PP nanocomposites as a function of Al nanoparticle volume fraction. Each permittivity is calculated from average capacitance measurements on at least five devices on at least two different thin films; error bars are included for each point, and the solid line is the percolation theory fit for the composites below the critical threshold [75]. Reproduced with permission from Fredin et al. Advanced Functional Materials 2013, 23, 3560–3569

the inclusion of inorganic fillers (e.g., metal oxides); and the addition of small molecules with a large permanent dipole moment that act as dielectric probes.

2. These approaches have enabled a wide range of dielectric studies on polyethylene and polypropylene and provided insights on the molecular origins of the main dielectric relaxations ($\alpha, \beta, \gamma, \delta$), in some cases aided by complimentary mechanical experiments. Moreover, the introduction of dipoles has allowed the monitoring of additional molecular processes, such as the entanglement formation dynamics in ultra-high molecular weight polyethylene (UHMWPE).
3. Polyolefin composites are of great relevance in electrical energy storage and insulation applications, as it is possible to tune their properties by combining the high permittivity and low dielectric losses of the polymer with the right choice of filler properties. The orientations of the polymer crystals, as well as filler orientation and hydrophilicity, have a strong influence on the final dielectric properties, for example, the higher orientation the larger the dielectric breakdown strength.

References

1. Plastics Europe (2018) Plastics—the Facts
2. Plastics Europe (2015) Plastics—the Facts
3. Schönhals A, Kremer F (2003) Broadband dielectr. Spectrosc 59
4. Boyd RH (1985a) Polymer 26:1123
5. Boyd RH, Gee RH, Han J, Jin Y (1994) J Chem Phys 101:788
6. Jourdan C, Cavaille JY, Perez J (1989) J Polym Sci Part B Polym Phys 27:2361

7. Suljovrujic E, Trifunovic S, Milicevic D (2010) Polym Degrad Stab 95:164
8. Tiemblo P, Gómez-Elvira JM, García Beltrán S, Matisova-Rychla L, Rychly J (2002) Macromol. 35:5922
9. Frübing P, Blischke D, Gerhard-Multhaupt R, Khalil MS (2001) J Phys D Appl Phys 34:3051
10. Drakopoulos SX, Psarras GC, Forte G, Martin-Fabiani I, Ronca S (2018) Polymer 150:35
11. Kakizaki M, Kakudate T, Hideshima T (1985) J Polym Sci Polym Phys Ed 23:809
12. Stamboliev G, Suljovrujic E (2010) Polym Degrad Stab 95:593
13. Quijada-Garrido I, Barrales-Rienda JM, Pereña JM, Frutos G (1997) J Polym Sci Part B Polym Phys 35:1473
14. Suljovrujic E (2012) Polym Bull 6:2033
15. Starkweather HW, Avakian P, Matheson RR, Fontanella JJ, Wintersgill MC (1992) Macromolecules 25:6871
16. Boyd RH (1985b) Polymer 26:323
17. Wunderlich B (2003) Prog Polym Sci 2:383
18. Stehling FC, Mandelkern L (1970) Macromolecules 3:242
19. Lee H, Cho K, Ahn T, Choe S, Kim I, Park I, Lee BH (1997) J Polym Sci Part B Polym Phys 3:1633
20. Vlassopoulos D (2006) Eur Phys J E 19:113
21. Alberola N, Cavaille JY, Perez J (1992) Eur Polym J 2:949
22. Cooper JW, Mccrum NG (1972) J Mater Sci 7:1221
23. McCrum NG, Read BE, Williams G (1967) Anelastic and dielectric effects in polymer solids. Wiley, London
24. Ashcraft CR, Boyd RH (1976) J Polym Sci Polym Phys Ed 1:2153
25. Gilchrist JLG (1978) J Polym Sci Polym Phys Ed 16:1773
26. Phillips WA (1970) Proc R Soc A Math Phys Eng Sci 319:565
27. Milicevic D, Micic M, Suljovrujic E (2014) Polym Bull 7:2317
28. Suljovrujic E (2009) Polym Degrad Stab 9:521
29. Ribes-greus A, Calleja RD (1989) 38:1127
30. Olivares N, Tiemblo P, Gómez-Elvira JM (1999) Polym Degrad Stab 6:297
31. Livanova NM, Zaikov GE (1997) Oxid Commun 2:443
32. Ramanujam M, Wachtendorf V, Purohit PJ, Mix R, Schönhals A, Friedrich JF (2012) Thermochim Acta 530:73
33. Roe RJ, Gieniewski C (1973) Macromolecules 6:212
34. Rastogi S, Lippits DR, Peters GWM, Graf R, Yao Y, Spiess HW (2005) Nat Mater 4:635
35. Romano D, Andablo-Reyes E, Ronca S, Rastogi S (2015) Polymer 74:76
36. Ferry JD (1980) Viscoelastic properties of polymers, 3rd edn. Wiley, New York
37. Liu K, de Boer EL, Yao Y, Romano D, Ronca S, Rastogi S (2016) Macromolecules 49:7497
38. Adachi K, Kotaka T (1987) J Mol Liq 3:75
39. Van Den Berg O, Sengers WGF, Jager WF, Picken SJ, Wübbenhorst M (2004) Macromolecules 37:2460
40. Sengers WGF, Van Den Berg O, Wübbenhorst M, Gotsis AD, Picken SJ (2005) Polymer 46:6064
41. Simon P, Gogotsi Y, Dunn B (2014) Science (80–) 343:1210
42. Presser V, Dennison CR, Campos J, Knehr KW, Kumbur EC, Gogotsi Y (2012) Adv Energy Mater 2:895
43. Tomer V, Polizos G, Randall CA, Manias E (2011) J Appl Phys 1:074113
44. Jiang J, Zhang X, Dan Z, Ma J, Lin Y, Li M, Nan C-W, Shen Y, Appl ACS (2017) Mater Interfaces 9:29717
45. Hao X (2013) J Adv Dielectr 0:1330001
46. Chen Q, Shen Y, Zhang S, Zhang QM (2015) Annu Rev Mater Res 4:433
47. Yao Z, Song Z, Hao H, Yu Z, Cao M, Zhang S, Lanagan MT, Liu H (2017) Adv Mater 29s
48. Roy M, Nelson JK, MacCrone RK, Schadler LS, Reed CW, Keefe R, Zenger W (2005) IEEE Trans Dielectr Electr Insul 1:629
49. Tanaka T, Kozako M, Fuse N, Ohki Y (2005) IEEE Trans Dielectr Electr Insul 1:669

50. Ezquerra TA, Majszczyk J, Baltà-Calleja FJ, López-Cabarcos E, Gardner KH, Hsiao BS (1994) Phys Rev B 50:6023
51. Arous M, Ben Amor I, Kallel A, Fakhfakh Z, Perrier G (2007) J Phys Chem Solids 68:1405
52. Hozumi N, Ishida M, Okamoto T, Fukagawa H (1990) IEEE Trans Electr Insul 2:707
53. Rytöluoto I, Gitsas A, Pasanen S, Lahti K (2017) Eur Polym J 9:606
54. Luo X, Chung DD (1999) Compos Part B Eng 3:227
55. Psarras GC (2006) Compos Part a Appl Sci Manuf 3:1545
56. Lux F (1993) J Mater Sci 2:285
57. Connor MT, Roy S, Ezquerra TA, Baltá Calleja FJ (1998) Phys Rev B 57:2286
58. Tsangaris GM, Psarras GC, Kouloumbi N (1998) J Mater Sci 3:2027
59. Pourrahimi AM, Olsson RT, Hedenqvist MS (2018) Adv Mater 3:1
60. Ayoob R, Alhabill F, Andritsch T, Vaughan A (2018) J Mater Sci 5:3427
61. Li B, Xidas PI, Manias E (2018) ACS Appl Nano Mater acsanm.8b00671
62. Ronca S, Igarashi T, Forte G, Rastogi S (2017) Polymer 123:203
63. Hosier IL, Praeger M, Vaughan AS, Swingler SG (2017) IEEE Trans Dielectr Electr Insul 2:3073
64. Wang W, Min D, Li S (2016) IEEE Trans Dielectr Electr Insul 2:564
65. Li B, Xidas PI, Triantafyllidis KS, Manias E (2017) Appl Phys Lett 1:082906
66. Yahagi K (1980) IEEE Trans Electr Insul EI-15 241
67. Linares A, Canalda JC, Cagiao ME, Garcia-Gutiérrez MC, Nogales A, Martín-Gullón I, Vera J, Ezquerra TA (2008) Macromolecules 41:7090
68. Nash JL (1988) Polym Eng Sci 2:862
69. Rabuffi M, Picci G (2002) IEEE Trans Plasma Sci 3:1939
70. Ajji A, Dumoulin MM, In Karger-Kocsis J ed (1999) Springer Netherlands, Dordrecht, pp 60–67
71. Virtanen S, Ranta H, Ahonen S, Karttunen M, Pelto J, Kannus K, Pettersson M (2014) J Appl Polym Sci 1:1
72. Bánhegyi G, Karasz FE (1987) Colloid Polym Sci 2:394
73. Etelaaho PJP, Haveri S (2011) Polym Compos 3:464
74. Zheng MS, Zheng YT, Zha JW, Yang Y, Han P, Wen YQ, Dang ZM (2018) Nano Energy 48:144
75. Fredin LA, Li Z, Lanagan MT, Ratner MA, Marks TJ (2013) Adv Funct Mater 2:3560